EEET ECOLOGICAL ENGINEERING & ENVIRONMENTAL TECHNOLOGY

Ecological Engineering & Environmental Technology 2022, 23(5), 1–19
https://doi.org/10.12912/27197050/151627
ISSN 2719-7050, License CC-BY 4.0

Received: 2022.06.21
Accepted: 2022.07.16
Published: 2022.08.01

Power Quality Enhancement of Smart Home Energy Management System in Smart Grid Using MAORDF-CapSA Technique

Vinjamuri Usha Rani[1,2*], Loveswara Rao Burthi[3]

[1] Koneru Lakshmaiah Education Foundation, Green Fields, Vaddeswaram, Andhra Pradesh 522502, India
[2] Department of Electrical and Electronics Engineering, Gokaraju Rangaraju Institute of Engineering and Technology, Bachupally, Survey No. 288, Nizampet Rd, Kukatpally, Hyderabad, Telangana 500090, India
[3] Department of Electrical and Electronics Engineering, Koneru Lakshmaiah Education Foundation, Vaddeswaram, Andhra Pradesh 522502, India
* Corresponding author's e-mail: ushakiran295@gmail.com

ABSTRACT
An IoT-based smart home energy management system (SHEMS) with power quality control (PQC) in Smart Grid using MAORDF-CapSA system is proposed in this paper. The proposed hybrid system is the combined execution of the Mexican axolotl optimization (MAO)-random decision forest (RDF) and the capuchin search algorithm (CapSA) therefore it is known as MAORDF-CapSA system. The main contribution of this paper is divided into two phases namely, smart home energy management system and power quality enhancement (PQE). In the first phase, the main objective of the proposed work is pointed out as it pursues: (1) to propose an energy management system for the distribution system that uses the IoT framework; (2) to deal with the power and resources of the distribution system; (3) promote the advancement of the demand response energy management system; (4) expand the adaptability of networks and optimize the use of accessible resources. The second phase permits to improve the shared use of the grid to maintain the power quality. The proposed CapSA controller detects the event of power quality issue and voltage rise. Additionally, the proposed system is responsible for meeting the general supply and energy demand. The performance of the proposed system is executed on the MATLAB platform and compared with various existing systems.

Keywords: energy management system, smart home energy management system, power quality control, high voltage alternative current.

INTRODUCTION

Sinusoidal current and voltage waveforms are great interest to the power system community, since power system equipment is designed to work at the important power frequency. Depending on the combination of non-linear loads like power electronics, static VAR compensators, converters and arc furnaces they may be equivalent or odd harmonics in the electrical system. Harmonic distortion caused by numerous non-linear loads on the power grid can lead to unfavorable issues (Addelaziz et al., 2011; Trianni et al., 2016). Depending on the power system, poor quality transformers, rotating devices, neutral conductors can affect the reliability and performance (Tao et al., 2014). To address this issue, international standards describe the maximal permissible limits for harmonic distortion levels (Bi et al., 2014; Tao et al., 2014). Power system operators improve its operating approaches depends on IEEE 519 or IEC 61000 standards. Based on the IEEE standard, 519-2014, the current distortion restricts the total demand distortion (TDD). In this literature, there are various executions to mitigate the effects of harmonics. In the middle of line reactors, phase shifting transformers, K-factor transformers, hybrid, passive and active low-pass harmonic filters have delivered (Siano, 2014; Marzband et al., 2013). The subprograms of DSM like load

shifting, peak clipping, are usually utilized for different purposes; load shifting can be assessed as most hopeful solutions to diminish harmonic distortions (Marband et al., 2014; Neves et al., 2015).

In this literature, power systems caused by harmonics from household appliances have been observed on several studies. In (Ding et al., 2014; Kondili et al., 1993; Ferrari et al., 2006; Jamsen et al., 2004; Erwinski et al., 2012; Figueriredo et al., 2005), measurements of current harmonics and analysis of its components are carried out for certain sorts of loads in high, medium and low voltage. Sources of harmonic generation and relevant standards are also deliberated. Many home appliances have a non-sinusoidal power converter increases the harmonic voltage level and enhances the overall effect and the harmonic diversity (Espinoza et al., 2005). Displacement power factor, transient currents and THD for Indian scenario are experimentally observed (Albert and Rajagopal, 2013). In Ahmad et al. (2012) measurements of current harmonics and analysis of its components for household appliances are carried out. Harmonic investigations of residential, commercial and industrial loads on North America are carried out through analyses of data collected from several distribution systems and third harmonic. To control the harmonic level of network depends on harmonic pricing is proposed through the aim of giving fair harmonic pricing allocation. The paybacks of DSM or their sub-branch load shifting are not deemed for the purpose of decreasing harmonics. In Moro et al. (2014), the economic effect of load shifting is explored by modeling the appliances utilized at typical household. Furthermore, load shifting is used in research to restore consumer habits. When DSM or load shifting is involved, harmonic mitigation (Wu et al., 2014) is not taken into account.

This paper proposes an IoT based smart home energy management system (SHEMS) with power quality control (PQC) in smart grid using MAORDF-CapSA system. The proposed hybrid system is the combined execution of Mexican axolotl optimization (MAO), random decision forest (RDF) and capuchin search algorithm (CapSA) and hence it is named as MAORDF-CapSA method.

BACKGROUND

Various research works have earlier existed in the literatures which are based on the smart home energy management with power quality enhancement using various methods and features. Some of them are revised here.

Rodrigues Junior et al. (2021) have illustrated a low-voltage measurement hardware uses an ARM Cortex M4 and real-time operating system. The proposed metering infrastructure was utilized as a smart meter, providing power quality monitoring service. Nevertheless, managing an extensive range of operations was complex task. To overwhelm this difficulty, the use of a real-time operating system delivered by Texas Instruments (named TI-RTOS) was suggested. Therefore, a low computational cost methodology was defined and incorporated. Karthick and Chandrasekaran (2021) have provided a novel commercial building energy management system (CBEMS) uses smart compact energy meter (SCEM)-fed IOT. Here, the low-voltage measurement hardware utilizes the Cortex of Machines and the advanced reduced instruction set computing (RISC) real-time operating system. The selection of ARM microprocessor aims to execute an extensive range of complex operations.

Wang et al. (2021) have described a novel optimal method for HEMS depends on IoT. This system was multi-objective optimization process deliberates two key purposes, together with the cost of energy consumption and user satisfaction. The users' impact on system efficiency based on energy cost savings was important. The IoT system was depends on ZigBee. Suja (2021) had illustrated Levy's flight moth flame optimization (LFMFO) to improve performance and diminish PQ issues on SG system. The presented approach was authenticated on the MATLAB/Simulink platform. The presented system displays the capability to alleviate PQ problems on SG system. The presented systems deliver the best optimal result to attain the objective of the MG system.

Duman et al. (2021) have postulated combining a smart thermostat with HEMS. The MILP-fed HEMS executes load scheduling to minimize costs and delivers optimal demand response (DR) and photovoltaic (PV) DR air conditioning and maintenance of thermal comfort. At initial phase, the proposed thermostat describes dissimilar set points for every time interval. At second phase, the HEMS programs the operation of the loads with time change, thermostatic control and power change. Javadi et al. (2021) had introduced a self-programming model for HEMS creation of a linear discomfort index (DI) incorporates the preferences of end users on daily operation. The proposed DI regulates the

optimal time intervals for the operation of household appliances and minimizes the bills of the end users. The resulting multi-objective optimization issue was solved by the epsilon restriction system and the VIKOR decision maker was used to choose the most preferred Pareto solution. Rehman et al. (2021) have introduced load scheduling and energy storage system management controller (LSEMC) was depends on heuristic algorithms i.e., genetic algorithm (GA), wind driven optimization (WDO), binary particle swarm optimization (BPSO). The performance of heuristic algorithms and proposed system was assessed mathematically.

Motivation for the research work

The review of current research work displays that the SHEMS, as well as the improvement in power quality, is the main task. In the literature, smart sensors may be deemed necessary IoT devices for smart grids. Smart sensors deliver approximate information to drive information and detailed analysis. The main objectives create technical fixes to attain accuracy for unusual situations and to recover the quality and reliability of the system. In the future, IoT desires to maximize customer satisfaction and business efficiency. The IoT-fed framework should have the capability to handle and change in response to those changes for the application of the IoT framework at the right time. This system has two units: the director of resources and the director of autonomy. The sensor detects nature and gathers information. Sensor detectors are an interface that smart devices use to monitor the land. The information is detached, monitored and then disclosed. At transmission and distribution monitoring systems, smart sensors may be utilized in several places. It distributes them to networks like power grids, distribution lines, etc. It has two sorts of smart sensors that may be utilized to measure weather conditions around benefits like wind direction sensors, temperature sensors, wind speed sensors, etc. These sensors are in charge for the help and mitigation of violent incidents using the current network. These drawbacks and motivations are inspired to do this research work.

DESIGN OF IoT BASED SHEMS IN SMART GRID

Smart home energy management provides the advanced configuration of IoT technology with the possibility for transforming the traditional home into a smart energy aware environment for managing the demand resource and the energy resource is used to diminish excess energy consumption. The coordinated framework with core intelligence is used to mechanize, expedite and coordinate decision-making on smart home product ecosystem in the absence of considering occupant involvement.

Current smart home energy management implements the different types of intelligent controllers that need exterior feedback of input values like cost, demand, thermal and photovoltaic generations. Smart home energy management may be classified into two main types depends on the levels of intelligence they provide to automate energy demand and control task usage. These controllers fall into two categories depends on the majority level of intelligence delivered to the system.

For utilizing equipment quickly with greater energy saving potential, this is necessary when the occupants want to use it. For instance, when turning on low-ventilation HVAC equipment, the priority rate is used for the specified periods. This consumes less energy likened to operating HVAC equipment is on high ventilation at the rate at which demand rises. The general architecture of the SHEMS portrays on Figure 1.

The analytical controller is designed to automate the on/off of appliances. The derived model is simulated in Energy Plus software compared to a traditional thermostat, considerably reduces excess energy. To modify seat temperature, points are depend on indoor weather conditions and the capability. In some cases are used to improve the reliability of smart home energy management. Activities are considered when formulating behavior towards energy demand and use. To manage the home appliance the dynamic predictive controls are utilized which is not based on the occupants fixed schedule.

Objective

A novel scheme is presented that classifies the load obtainable on locality into primary and secondary loads. Some examples, such as the fan, universal serial bus (USB) lights, and charger, are deemed primary loads, while the air conditioner is deemed from secondary load.

Power consumption and power quality disturbances

Incoming power is initially detected using a voltage sensor and a current sensor to maintain

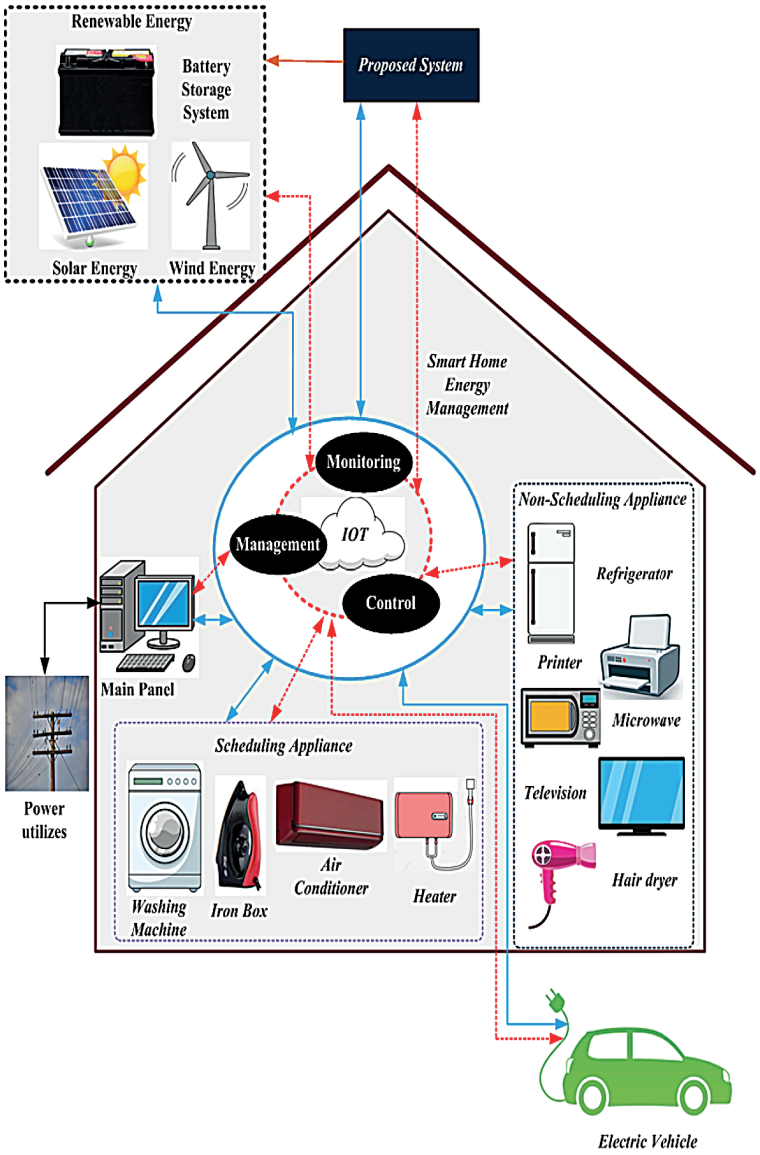

Figure 1. General architecture of SHEMS

the power quality. While the current sensor and voltage sensors are placed in series with the supply. The representation diagram of power quality (PQ) disturbance monitoring system portrays on Figure 2.

Voltage and current values

RMS values are computed from voltage sensor and current sensor to monitor power quality distribution are described below:

$$V_{RMS} = \sqrt{\frac{1}{t}\int_0^t V^{"2}(T)\,DT} \tag{1}$$

$$I_{RMS} = \sqrt{\frac{1}{t}\int_0^t I^{"2}(T)\,DT} \tag{2}$$

where: the *V"* is represent as voltage signal received from the voltage sensor and *I"* is represent as current signal received from the voltage sensor.

Real and reactive power values

The real and reactive power are described on equation 3 and 4:

$$p = \frac{1}{n}\sum_{N=1}^{n} V(M)\,I(M) \tag{3}$$

where: *V(M)* denoted as sampled example of *V(T)*, *I(M)* represent as sampled example of *I(T)*, *M* signifies the number of samples.

$$q = V_I I_1 sin\varphi \tag{4}$$

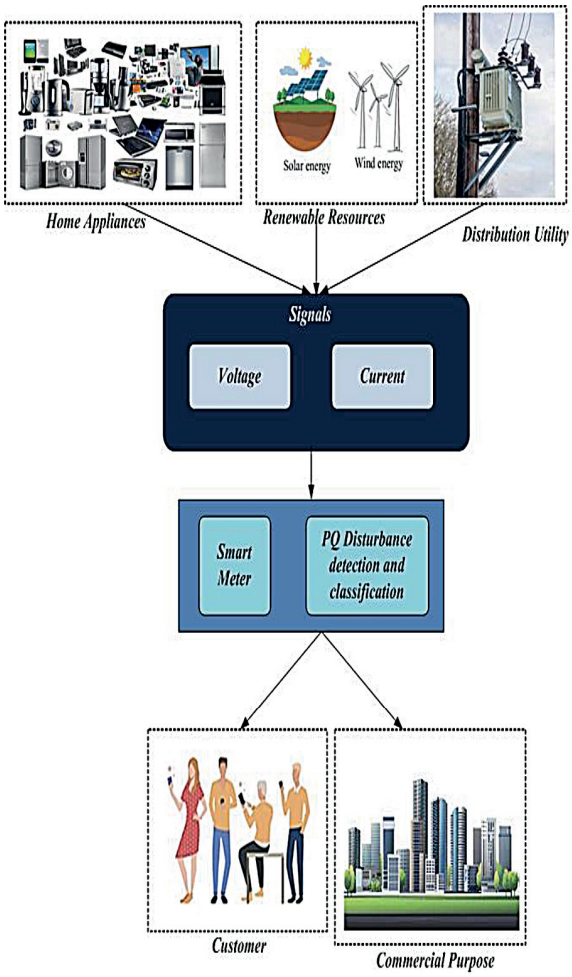

Figure 2. Representation diagram of the PQ disturbance monitoring system

RMS current

RMS current values are measured with Eq. 5:

$$RMS_I = \sqrt{\frac{1}{n} * \sum_{J=1}^{n} D_{IJ}^2} \tag{5}$$

where: $D_{IJ} = -J$ is the point of voltage.

Total harmonic distortion values

Total harmonic distortion (THD) provided with Equation 6:

$$THD_I = 100 * \sqrt{\frac{\sum_{k=2}^{25} x_k^2}{x_1}} \tag{7}$$

where: I is denoted as the size.

Euclidean distance

Euclidean distance is utilized to compute the degree of similarity since it is generally utilized. Every feature are extracted as analyzed window, the below Euclidean distance (d_I) is computed:

$$d_I = \sqrt{\left(X_{Ref} - X_I\right)^2} \tag{7}$$

where: X_{Ref} is denoted as the THD values.

PROPOSED ALGORITHM MAORDF-CapSA TECHNIQUE

The MAO algorithm is stimulated by birth, reproduction and tissue restoration of the axolotl, as well as the way they live on aquatic environment. RDF is a machine learning system for regression and classification issues that creates prediction model under the form of ensemble of weak forecast models, naturally decision trees.

Mexican axolotl optimization algorithm

The Mexican axolotl optimization (MAO) algorithm is the metaheuristic algorithm inspired by the axolotl life (Karthick et al 2021; Cicek et al 2021; Villuendas et al 2021). It is stimulated by birth, rearing and restoration of axolotl tissues. Since axolotls are sexual living being, the population is separated into males and females. In this work, the loss is minimized by means of the algorithm for the power extraction and increase the efficiency of proposed system. The step by step method is defined below:

- Step 1: Initialization

Here the input parameters such as wind energy, photovoltaic system, battery storage system and micro turbine.

- Step 2: Random Generation

To generate the population on random method.

- Step 3: Fitness calculation

It is based on the objective function, in which the loss of the system is minimized.

$$F_c = Min\left(P_L^*\right) \tag{8}$$

- Step 3: Organization of male female population

The individuals are allocated as male and female because the axolotls develop based on its sex.

- Step 4: Transition from larvae to adult state,

The male individuals will make the transition on the water, from larvae to adults, adjusting the color of its body parts towards the male that best suits the environment.

$$p(N,F)_j = \frac{Obj(N_j,F_j)}{\sum Obj(N_j,F_j)} \quad (9)$$

Modernize male and female populations

The probability value of male is superior to random value then updates the male population by,

$$N_{ji} = N_{ji} + N_{best,i} - N_{ji} * \alpha \quad (10)$$

Otherwise,

$$N_{ji} = Min_i + Max_i - Max_j * R_i \quad (11)$$

While, male axolotl represents M_j, random number as R_i:

$$F_{ji} = F_{ji} + F_{best,i} - F_{ji} * \alpha \quad (12)$$

Otherwise,

$$F_{ji} = Min_i + (Max_i - Max_i) * R_i \quad (13)$$

Flow chart of MAO is portrays on Figure 3.

- Step 5: Injury and restoration process

It may cause accidents and injuries. The probability is that the area is lost when damaged.

$$\bar{P}_{ji} = Min_i + (Max_i - Max_i) * R_i \quad (14)$$

- Step 6: Process of reproduction and Assortment

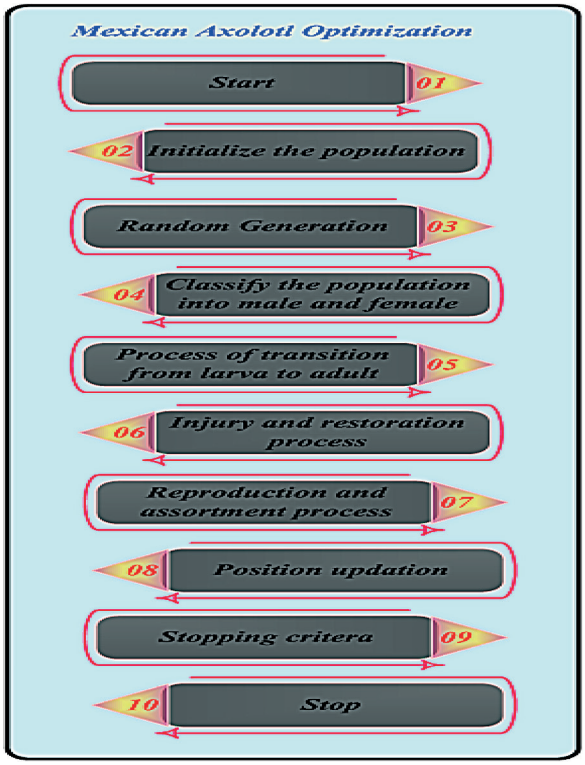

Figure 3. Flow chart of Mexican axolotl optimization algorithm

The male lays sperm and the female takes glucose to place in sperm. If the young larvae are better, it will be transplanted to a better condition.

- Step 7: Termination criteria

If the end criteria are fulfilled then find the optimal solution otherwise go to step 3.

Random decision forest

RDF is a group machine learning process that involves a computational process. RDF has two hyper parameters: the number of splits on sub-group at every end and trees on forest. Meanwhile, two problems can be seen (Rao et al 2019). Training models are randomly chosen at initial problem. At second complexity, each of the trees on forest is maximal. The step by step method of RDF displays below. Structure of the RDF portrays on Figure 4.

- Step 1: The first step of RDF is initialization of parameter like power demand
- Step 2: The RDF classifier system is generated by the combination of decision trees. Initially, Y numbers of trees on forest are deemed to create the decision tree:

$$Y = \{x_1(t), x_2(t), \cdots x_n(t)\}$$

- Step 3: The RDF is trained depends on input and target.
- Step 4: The significance of the variable is determined by comparing the prediction error

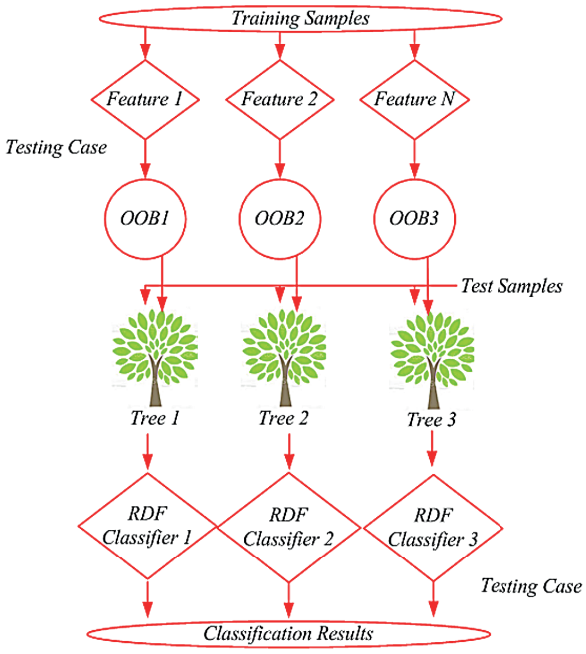

Figure 4. Structure of RDF

through the out-of-Bag data period. The OOB error of the target is computed from below:

$$OOB_{error} = W^{RDF(tar)} - W^{RDF(out)} \quad (15)$$

Each sample handles multiple data sets.

- Step 5: To increase the accuracy of the prediction.

$$V_I^{(tr)} = \frac{1}{T}\left(\frac{\sum_{xa\in\varphi^{c(tr)}} I(l_b = C_a^{tr}) - \sum_{xa\in\varphi^{c(tr)}} \sum_{xa\in\varphi^{c(tr)}} I(l_b = C_{a,nz}^{tr})}{\varphi^{c(tr)}}\right) \quad (16)$$

where: $\phi^{c(tr)}$ refers out-of-bag trail specimen for a peculiar tree, tree number denotes *tr*, the total number of tree represents *T*. If the variable importance declines, the precision will neither increase nor decrease. After the calculation of the VI, a similar number of elements are divided into the similar group using the density model cluster analysis system.

CapSA algorithm

The proposed scheme is a capuchin search algorithm (CapSA). The social structure of the capuchin monkey is arboreal, diurnal, highly territorial animals (Rao et al 2019).

- Step 1: Initialization of CapSA

The initial step of CapSA is the initialization of parameter such as K_P and K_I

$$X = \begin{bmatrix} X_1^1 & X_1^1 \ldots\ldots\ldots\ldots X_D^1 \\ X_1^2 & X_2^2 \ldots\ldots\ldots\ldots X_D^2 \\ \vdots & \vdots \quad\quad\quad\quad\quad \vdots \\ X_1^N & X_2^N \ldots\ldots\ldots\ldots X_D^N \end{bmatrix} \quad (17)$$

where: *X* refers positions of capuchins, n denotes number of capuchins and X_D^1 refers D^{th} dimension of position .

- Step 2: Random generation

In random generation, the input parameters are randomly generated in this step.

- Step 3: Fitness assessment

The fitness function of every cappuccino is evaluated by setting the values of the decision variables to a user-defined fitness function.

$$F = \begin{bmatrix} F_1\left(X_1^1 & X_1^1 \ldots\ldots\ldots\ldots X_D^1\right) \\ F_2\left(X_1^2 & X_2^2 \ldots\ldots\ldots\ldots X_D^2\right) \\ \vdots & \vdots \quad\quad\quad\quad\quad \vdots \\ F_N\left(X_1^N & X_2^N \ldots\ldots\ldots\ldots X_D^N\right) \end{bmatrix} \quad (18)$$

- Step 4: Initial location

Equation 19 may be utilized to assign the initial location:

$$X^I = UB_J + R \times \left(UB_J - LB_J\right) \quad (19)$$

where: LB_j and UB_j refers lower and upper bounds of i[th] capuchin oNj[th] dimension. Flow chart of CapSA-WHO is shown on Figure 5.

- Step 5: Evolutionary process of CapSA

The evolutionary process of CapSA is based on current and optimal levels of capuchins and the food source labeled *F*. The mathematical model describing the dynamic behavior of the leader alpha and its novel positions is revealed as follows.

a) Jumping of trees

Alpha capuchins jump tree to tree or tree branch to another branch of similar tree.

$$X_J^I = f_J + \frac{p_{BF}\left(V_J^I\right)^2 sin(2\theta)}{G} \quad (20)$$
$$I < M/2; 0.1 < \epsilon \leq 0.20$$

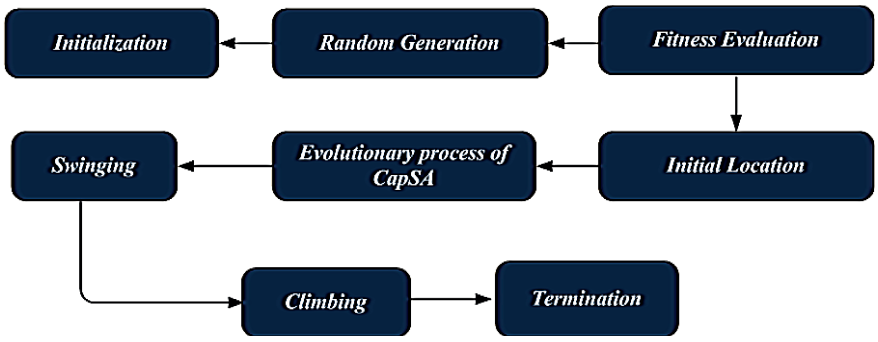

Figure 5. Flow chart of CapSA-WHO

where: X_J^I refers position of the alpha capuchins, θ implies jumping angle of the capuchins, V_J^I refers velocity of ith capuchin on j^{th} dimension and G refers gravitational force similar to 9.81.

b) Jumping angle

The jumping angle of capuchins may be provided as

$$\theta = \frac{3}{2}R \tag{21}$$

where: R refers random number created uniformly on interval [0, 1].

c) Life time of CapSA

A lifetime exponential function, τ, is proposed on CapSA among exploration and exploitation.

$$\tau = \beta_0 E^{\beta_1\left(\frac{1}{K}\right)^{\beta_2}} \tag{22}$$

where: k and K are denotes current and maximal values. The parameters β_0, β_1 and β_2 are arbitrarily selected as 2, 21 and 2.

d) Velocity of CapSA

The velocity of ith capuchin on jth dimension may be calculated as:

$$\begin{aligned} V_J^I &= \rho V_J^I + \tau A_I \\ &\left(X_{Best_J}^I - X_J^I\right) R_1 + \\ &\tau A_2 \left(f_J - X_J^i\right) R_2 \end{aligned} \tag{23}$$

where: A_1 and A_2 refers two positive constants, R_1 and R_2 are two random numbers created uniformly in the interval [0, 1].

e) Jumping on ground

Alpha Capuchins can jump one place to another, one side of a river to another, or they can simply walk in search of food. Capuchins use this behavior to travel long distances, especially when there is less food.

$$\begin{gathered} X_J^I = f_J + \frac{p_{EF} p_{BF} \left(V_J^2\right) sin(2\theta)}{G} \\ I < M/2; 0.2 < \epsilon \leq 0.30 \end{gathered} \tag{24}$$

where: p_{EF} denotes elasticity probability.

f) New location of alpha capuchins

The novel location of alpha capuchins utilizes normal walking may be computed from below:

$$\begin{gathered} X_J^I = X_J^I + V_J^I \\ I < N/2; 0.3 < \epsilon \leq 0.50 \end{gathered} \tag{25}$$

- Step 6: Swinging

Alpha capuchins and other sub-capuchins can utilize local food search to wander short distances on tree and the entire tree branches. They use its tails to catch the tree branch and swinging function to discover food sources on both sides of branch.

$$\begin{gathered} X_J^I = F_J + \tau p_{BF} \times sin(2\theta) \\ I < M/2; 0.5 < \epsilon \leq 0.75 \end{gathered} \tag{26}$$

- Step 7: Climbing

Alpha capuchins and other sub-capuchins can climb trees and their branches and descend from trees several times during a local food search-related activity.

$$\begin{gathered} X_J^I = F_J + \tau p_{BF} \times V_J^I - V_{J-1}^I) \\ I < M/2\,; 0.75 < \epsilon \leq 1.0 \end{gathered} \tag{27}$$

where: V_J^I refers current velocity of ith capuchin on jth dimension and $V_{J\text{-}1}^I$ refers earlier velocity of ith capuchin on jth dimension.

- Step 8: Termination

Check the stopping criteria. If the best value is determined then discontinue the process. Or else go to step 3.

RESULTS DISCUSSION

The existing systems are fruit fly optimization (FFO), fruit fly optimization and random decision optimization (FORDF), improved artificial bee colony (IABC), squirrel optimization with gravitational search-added neural network (SOGSNN), radial basic function neural network opposition's crow search algorithm (RBFNOCS).

Analysis of 24-hour power usage by each appliance is shown in Figure 6. In fridge, the value of power is 5. In iron, the value of power is 58. In toaster, the value of power is 18. In kettle, the value of power is 47. In hair dryer, the value of power is 35. In television, the value of power is 4. In desktop, the value of power is 3. In monitor, the value of power is 2. In light, the value of power is 1. In hair straighter, the value of power is 1.5. In oven, the value of power is 49. In dish washer, the value of power is 42. In micro oven, the value of power is 27. In printer, the value of power is 1. In air conditioner, the value of power is 28. In washing machine, the value of power is 43. In vacuum cleaner, the value of power is 46. In laptop, the value of power is 7.

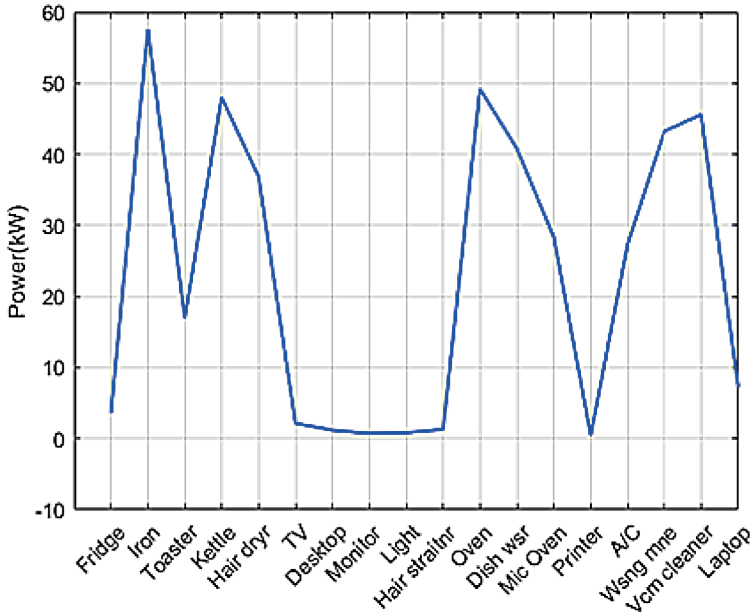

Figure 6. Analysis of 24-hour power usage by each appliance

Performance analysis of battery power and demand power for MAORDF-CapSA technique is shown in Figure 7. In battery, when the value of time is 5 then the value of power is 0.1. When the value of time is 10 then the value of power is 0.0098. When the value of the time is 15 then the value of power is 0.3. When the value of time of 20 then the value of power is 0.305. In demand, when the value of time is 5 then the value of power is 0.1. When the value of time is 10 then the value of power is 0.0099. When the value of the time is 15 then the value of power is 0.205. When the value of time of 20 then the value of power is 0.35.

Performance of battery-power is shown in Figure 8. When the value of power is 0.01 then the value of time is 5. When the value of power is 0.82 then the value of time is 7. When the value of power is 0.04 then the value of time is 10. When the value of power is 0.104 then the value of time is 15. When the value of power is 0.3 then the value of time is 20. When the value of power is 0.67 then the value of time is 25.

Figure 9 displays the cost & demand power MAORDF-CapSA. In left hand side of PV, when the value of cost is 0.01 then the value of time is 5. When the value of cost is 0.02 then the value of

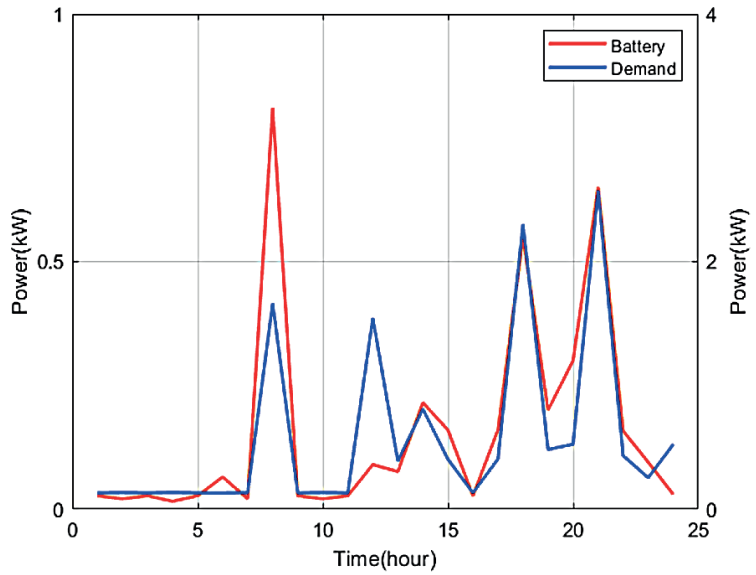

Figure 7. Performance analysis of battery power and demand power for MAORDF-CapSA technique

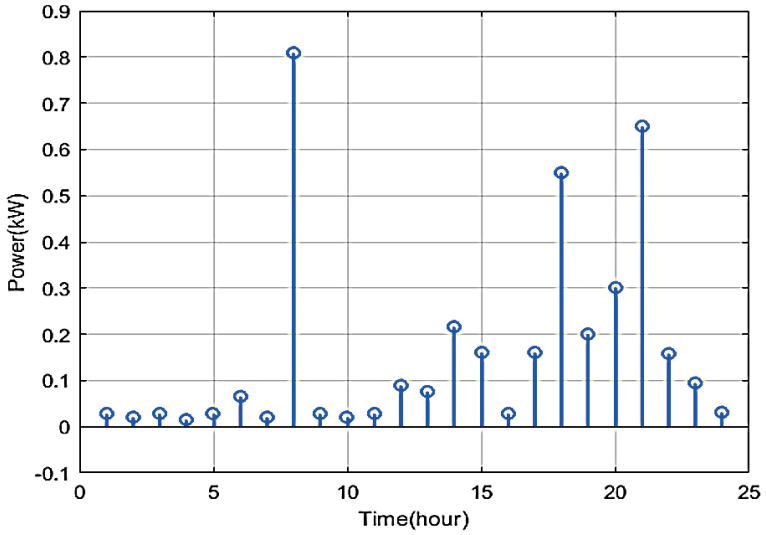

Figure 8. Performance of battery-power

time is 10. When the value of cost is 0.09 then the value of time is 15. When the value of cost is 0.04 then the value of time is 20. In demand, when the value of cost is 0.03 then the value of time is 5. When the value of cost is 0.106 then the value of time is 7. When the value of cost is 0.03 then the value of time is 10. When the value of cost is 0.06 then the value of time is 15. When the value cost is 0.07 then the value of time is 20. In demand when the value of cost is 0.09 then the value of time is from 2 to 7. When the value of cost is 0.105 then the value of time is 8. When the value of cost is 0.09 then the value of time is 10. When the value of cost is 0.103 then the value of time is 12. In demand, when the value of cost is 0.013 then the value of time is 15. When the value of cost is 0.203 then the value of time is 18. When the value of cost is 0.07 then the value of time is 20. When the value of cost is 0.209 then the value of time is 22. When the value of power and cost is 0.02 then the value of time is 24. When the value of time is 12 then the value of cost is 1.2. When the value of time is 15 then the value of cost is 0.07. When the value of time is 17 then the value of cost is 2.3. When the value of time is 17 then the value of cost is 1.7.

Comparison of (a) FFO with MAORDF-CapSA Technique, (b) FORDF with MAORDF-CapSA

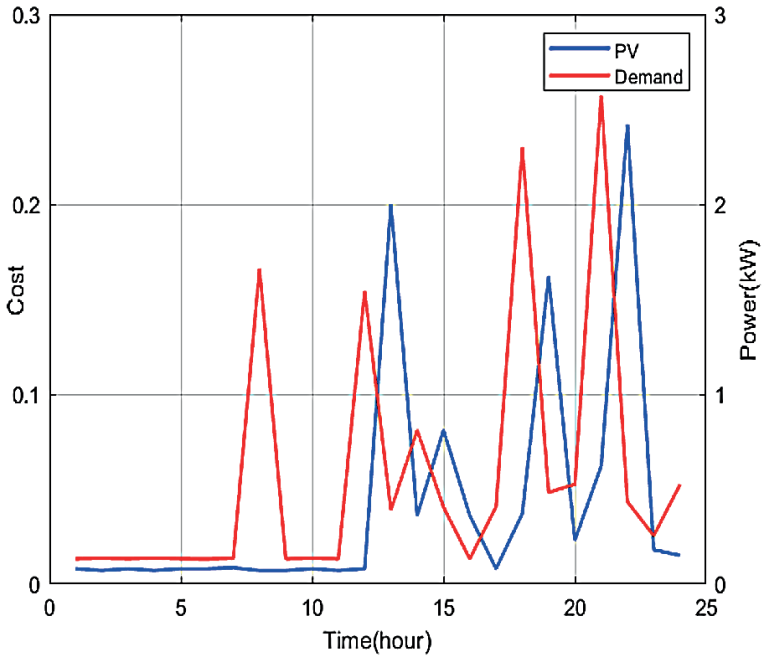

Figure 9. Cost & demand power MAORDF-CapSA

(c) GOAPSNN with MAORDF-CapSA (d) IABC with MAORDF-CapSA Technique, (e) RBFNOCS with MAORDF-CapSA (f) FORDF with SOG-SNN-CapSA Technique is shown in Figure 10. Comparison of FFO with MAORDF-CapSA Technique is shown in Figure 10(a). In FFO, when the value of cost is 5 then the value of time is 0.02. When the value of cost is 10 then the value

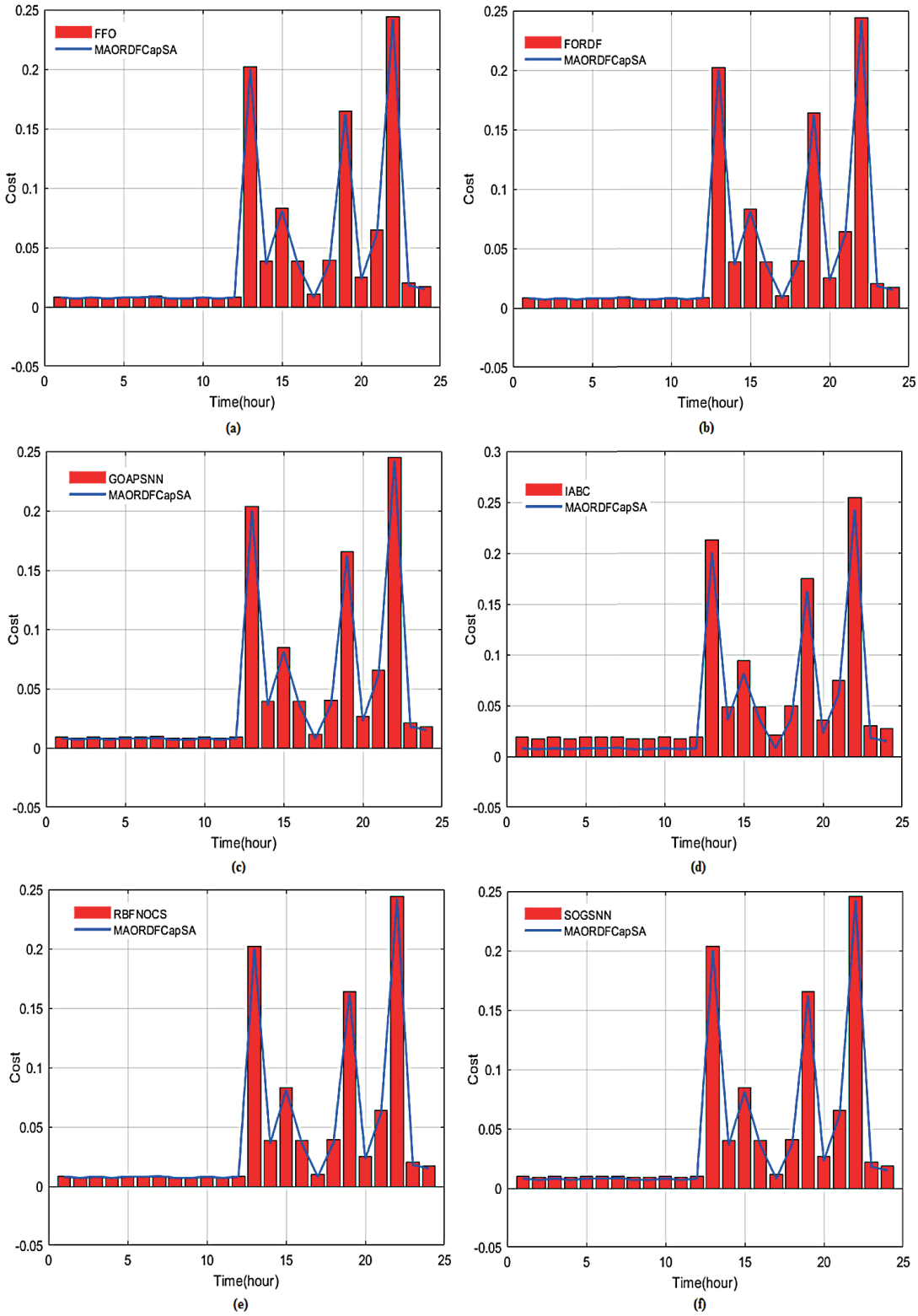

Figure 10. Comparison of (a) FFO with MAORDF-CapSA technique, (b) FORDF with MAORDF-CapSA (c) GOAPSNN with MAORDF-CapSA (d) IABC with MAORDF-CapSA (e) RBFNOCS with MAORDF-CapSA (f) FORDF with SOGSNN-CapSA

of time is 0.01. When the value of cost is 13 then the value of time is increases to 0.2. When the value of cost is 15 then the value of time is 0.07. When the value of cost is 20 then the value of time is decreases to 0.02. When the value of cost is 23 then the value of time is increases to 0.24. When the value of cost is 24 then the value of time is increases to 0.04. In MAORDF-CapSA technique, when the value of cost is 5 then the value of time is 0.01. When the value of cost is 10 then the value of time is 0.02. When the value of cost is 13 then the value of time is increases to 0.3. When the value of cost is 15 then the value of time is 0.08. When the value of cost is 20 then the value of time is decreases to 0.03. When the value of cost is 23 then the value of time is increases to 0.25. When the value of cost is 24 then the value of time is increases to 0.05. Comparison of FORDF with MAORDF-CapSA technique is shown in Figure 10(b). In FORDF, when the value of cost is 5 then the value of time is 0.03. When the value of cost is 10 then the value of time is 0.02. When the value of cost is 13 then the value of time is increases to 0.3. When the value of cost is 15 then the value of time is 0.08. When the value of cost is 20 then the value of time is decreases to 0.03. When the value of cost is 23 then the value of time is increases to 0.25. When the value of cost is 24 then the value of time is increases to 0.04. In MAORDF-CapSA technique, when the value of cost is 5 then the value of time is 0.02. When the value of cost is 10 then the value of time is 0.03. When the value of cost is 13 then the value of time is increases to 0.3. When the value of cost is 15 then the value of time is 0.09. When the value of cost is 20 then the value of time is decreases to 0.04. When the value of cost is 23 then the value of time is increases to 0.26. When the value of cost is 24 then the value of time is increases to 0.06. Comparison of GOAPSNN with MAORDF -CapSA technique is shown in Figure 10(c). In FORDF, when the value of cost is 5 then the value of time is 0.04. When the value of cost is 10 then the value of time is 0.03. When the value of cost is 13 then the value of time is increases to 0.4. When the value of cost is 15 then the value of time is 0.09. When the value of cost is 20 then the value of time is decreases to 0.04. When the value of cost is 23 then the value of time is increases to 0.26. When the value of cost is 24 then the value of time is increases to 0.05. In MAORDF-CapSA technique, when the value of cost is 5 then the value of time is 0.03. When the value of cost is 10 then the value of time is 0.04. When the value of cost is 13 then the value of time is increases to 0.3. When the value of cost is 15 then the value of time is 0.009. When the value of cost is 20 then the value of time is decreases to 0.05. When the value of cost is 23 then the value of time is increases to 0.27. When the value of cost is 24 then the value of time is increases to 0.07. Comparison of IABC with MAORDF-CapSA technique is shown in Figure 10(d). In FORDF, when the value of cost is 5 then the value of time is 0.03. When the value of cost is 10 then the value of time is 0.03. When the value of cost is 13 then the value of time is increases to 0.25. When the value of cost is 15 then the value of time is 0.09. When the value of cost is 18 then the value of time is 0.17. When the value of cost is 20 then the value of time is decreases to 0.04. When the value of cost is 24 then the value of time is increases to 0.05. In MAORDF-CapSA technique, when the value of cost is 5 then the value of time is 0.02. When the value of cost is 10 then the value of time is 0.02. When the value of cost is 13 then the value of time is increases to 0.2. When the value of cost is 15 then the value of time is 0.07. When the value of cost is 18 then the value of time is 0.16. When the value of cost is 20 then the value of time is decreases to 0.04. When the value of cost is 24 then the value of time is increases to 0.03. Comparison of RBFNOCS with MAORDF-CapSA technique is shown in Figure 10(e). In RBFNOCS, when the value of cost is 5 then the value of time is 0.02. When the value of cost is 10 then the value of time is 0.02. When the value of cost is 13 then the value of time is increases to 0.21. When the value of cost is 15 then the value of time is 0.07. When the value of cost is 18 then the value of time is 0.17. When the value of cost is 20 then the value of time is decreases to 0.02. When the value of cost is 23 then the value of time is increases to 0.24. When the value of cost is 24 then the value of time is increases to 0.04. In MAORDF-CapSA technique, when the value of cost is 5 then the value of time is 0.01. When the value of cost is 10 then the value of time is 0.02. When the value of cost is 13 then the value of time is increases to 0.3. When the value of cost is 15 then the value of time is 0.08. When the value of cost is 18 then the value of time is 0.16. When the value of cost is 20 then the value of time is decreases to 0.03. When the value of cost is 23 then the value of time is increases to 0.25. When the value of cost is 24 then the value of time is increases to 0.05. Comparison

of SOGSNIN with MAORDF-CapSA technique is shown in Figure 10(f). In SOGSNIN, when the value of cost is 5 then the value of time is 0.02. When the value of cost is 10 then the value of time is 0.02. When the value of cost is 13 then the value of time is increases to 0.21. When the value of cost is 15 then the value of time is 0.07. When the value of cost is 18 then the value of time is 0.17. When the value of cost is 20 then the value of time is decreases to 0.02. When the value of cost is 23 then the value of time is increases to 0.24. When the value of cost is 24 then the value of time is increases to 0.04. In MAORDF-CapSA technique, when the value of cost is 5 then the value of time is 0.01. When the value of cost is 10 then the value of time is 0.02. When the value of cost is 13 then the value of time is increases to 0.3. When the value of cost is 15 then the value of time is 0.08. When the value of cost is 18 then the value of time is 0.16. When the value of cost is 20 then the value of time is decreases to 0.03. When the value of cost is 23 then the value of time is increases to 0.25. When the value of cost is 24 then the value of time is increases to 0.05.

Performance analysis of demand power is shown in Figure 11. When the value of power is 5 then the value of time is 0.2. When the value of power is 7 then the value of time is 1.7. When the value of power is 10 then the value of time is 0.2. When the value of power is 12 then the value of time is 1.6. When the value of power is 14 then the value of time is 0.8. When the value of power is

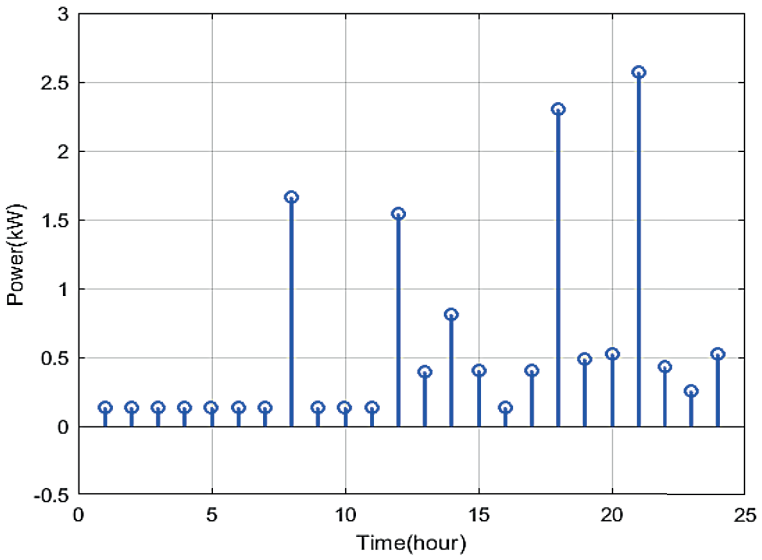

Figure 11. Analysis of demand power

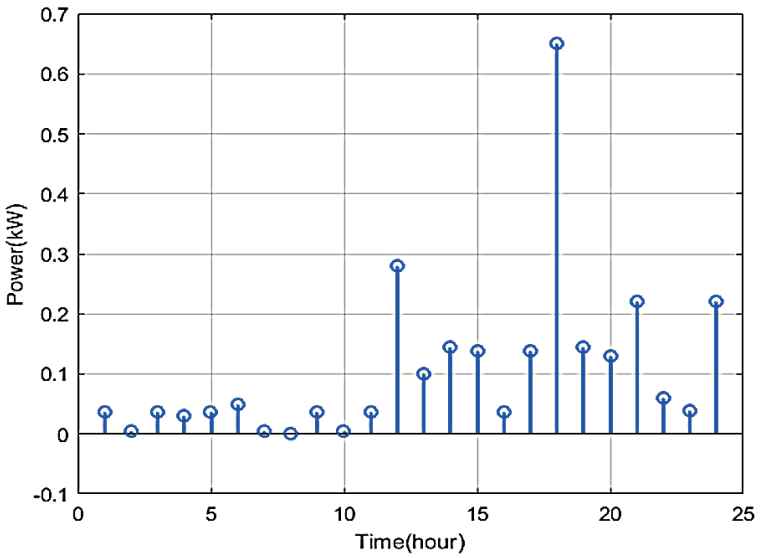

Figure 12. Analysis of demand power

15 then the value of time is 0.4. When the value of power is 17 then the value of time is 2.4. When the value of power is 20 then the value of time is 0.6. When the value of power is 21 then the value of time is 2.6. When the value of power is 24 then the value of time is 0.6.

Performance analysis of demand power is shown in Figure 12. When the value of power is 5 then the value of time is 0.3. When the value of power is 10 then the value of time is 0. When the value of power is 12 then the value of time is 0.29. When the value of power is 15 then the value of time is 0.15. When the value of power is 18 then the value of time is 0.65. When the value of power is 20 then the value of time is 0.15. When the value of power is 21 then the value of time is 0.22. When the value of power is 24 then the value of time is 0.22.

Analysis of MT & demand power proposed is shown in Figure 13. In left hand side of MT, when the value of power is 5 then the value of time is 0.1. When the value of power is 10 then the value of time is 0. When the value of power is 12 then the value of time is 0.304. When the value of power is 15 then the value of time is 0.201. When the value of power is 17 then the value of time is 0.604. When the value of power is 20 then the value of time is 0.203. When the value of power is 24 then the value of time is 0.301. In left hand side of demand, when the value of power is 5 then the value of time is 0.1. When the value of power is 7 then the value of time is 0.4. When the value of power is 10 then the value of time is 0.1. When the value of power is 12 then the value of time is 0.3. When the value of power is 14 then the value of time is 0.204. When the value of power is 15 then the value of time is 0.1. When the value of power is 17 then the value of time is 0.6. When the value of power is 20 then the value of time is 0.03. When the value of power is 22 then the value of time is 0.604. When the value of power is 24 then the value of time is 0.1. In right hand side of MT, when the value of power is 5 then the value of time is 0.1. When the value of power is 10 then the value of time is 0. When the value of power is 12 then the value of time is 1.7. When the value of power is 15 then the value of time is 0.6. When the value of power is 17 then the value of time is 2.3. When the value of power is 20 then the value of time is 0.4. When the value of power is 22 then the value of time is 2.4. When the value of power is 24 then the value of time is 1. In right hand side of demand, when the value of power is 5 then the value of time is 0.2. When the value of power is 7 then the value of time is 1.8. When the value of power is 10 then the value of time is 0.1. When the value of power is 12 then the value of time is 1.4. When the value of power is 15 then the value of time is 0.4. When the value of power is 17 then the value of time is 2.1. When the value of power is 20 then the value of time is 0.4. When the value of power is 22 then the value of time is 0.5. When the value of power is 24 then the value of time is 0.6.

Analysis of PV & demand power MAORDF-CapSA is shown in Figure 14. In left hand side of demand, when the value of power is 5 then the value of time is 0.1. When the value of power is 7 then the value of time is 0.4. When the value of power is 10 then the value of time is 0.1. When the value of power is 12 then the value of time is 0.035. When the value of power is 15 then the value of time is

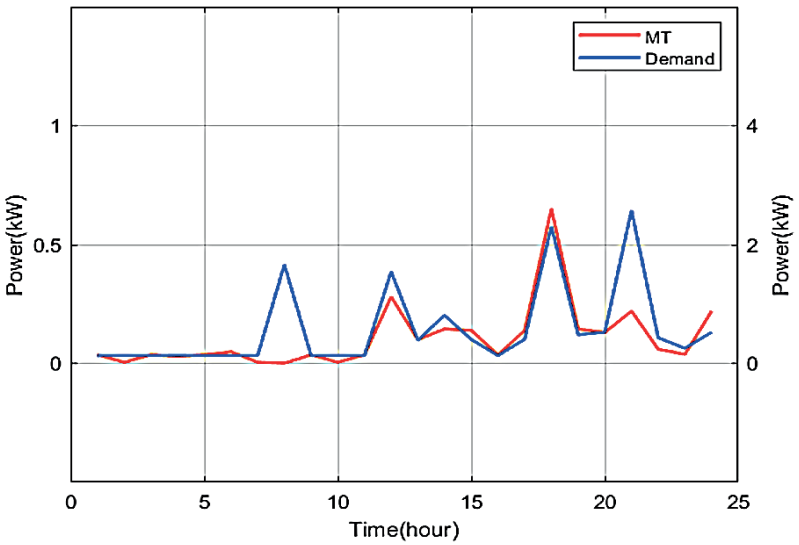

Figure 13. Analysis of MT & demand power proposed

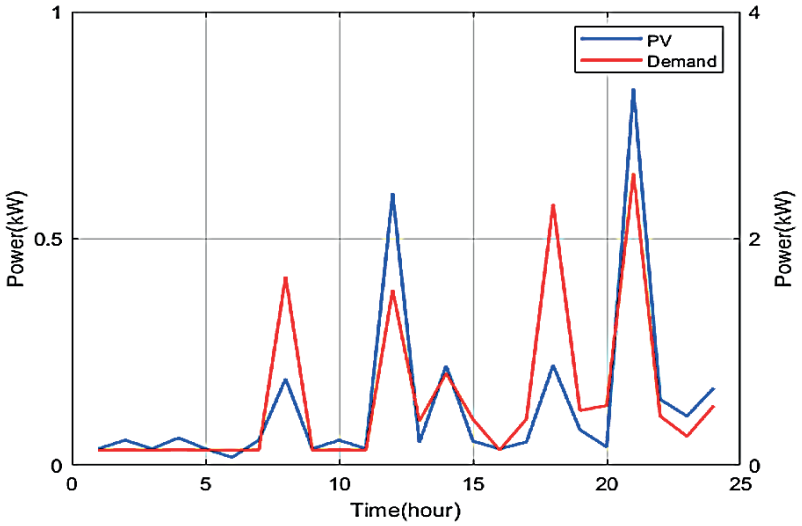

Figure 14. Analysis of PV & demand power MAORDF-CapSA

0.3. When the value of power is 17 then the value of time is 0.6. When the value of power is 20 then the value of time is 0.35. When the value of power is 21 then the value of time is 0.604. When the value of power is 23 then the value of time is 0.2. When the value of power is 24 then the value of time is 0.205. Then the value of time is 0.1. When the value of power is 7 then the value of time is 0.2. When the value of power is 10 then the value of time is 0.014. When the value of power is 12 then the value of time is 0.604. When the value of power is 15 then the value of time is 0.203. When the value of power is 17 then the value of time is 0.306. When the value of power is 20 then the value of time is 0.204. When the value of power is 21 then the value of time is 0.605. When the value of power is 23 then the value of time is 0.3. When the value of power is 24 then the value of time is 0.206. In right hand side of demand, when the value of power is 5 then the value of time is 0.1. When the value of power is 7 then the value of time is 1.8. When the value of power is 10 then the value of time is 0.1. When the value of power is 12 then the value of time is 1.7. When the value of power is 15 then the value of time is 0.9. When the value of power is 17 then the value of time is 2.3. When the value of power is 20 then the value of time is 2. When the value of power is 22 then the value of time is 2.5. When the value of power is 24 then the value of time is 0.8. In right hand side of PV, when the value of power is 5 then the value of time is 0.1. When the value of power is 7 then the value of time is 1. When the value of power is 10 then the value of time is 0.3. When the value of power is 12 then

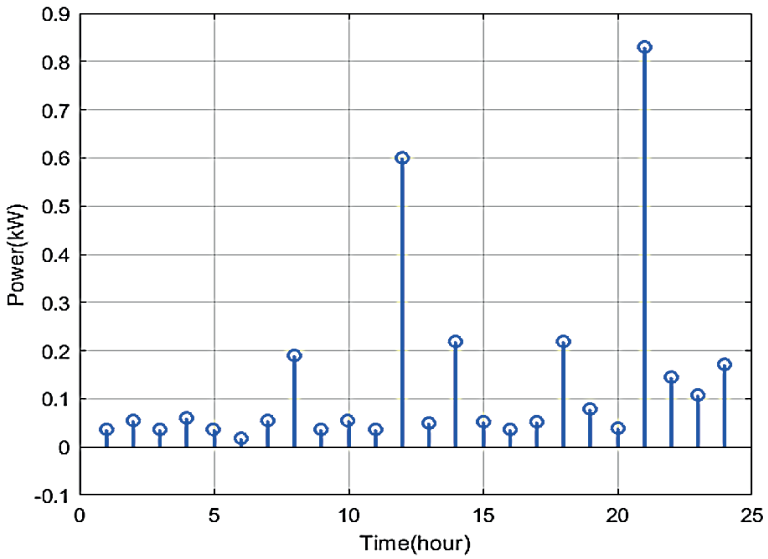

Figure 15. Analysis of PV power

the value of time is 2.3. When the value of power is 15 then the value of time is 0.5. When the value of power is 17 then the value of time is 1.6. When the value of power is 20 then the value of time is 0.1. When the value of power is 222 then the value of time is 3.2. When the value of power is 24 then the value of time is 0.9.

Figure 15 shows that performance analysis of PV power. When the value of power is 4 then the value of time is 0.7. When the value of power is 5 then the value of time is 0.02. When the value of power is 8 then the value of time is 0.09. When the value of power is 10 then the value of time is 0.008. When the value of power is 11 then the value of time is 0.6. When the value of power is 14 then the value of time is 0.202. When the value of power is 15 then the value of time is 0.005. When the value of power is 18 then the value of time is 0.203. When the value of power is 20 then the value of time is 0.004. When the value of power is 21 then the value of time is 0.83. When the value of power is 24 then the value of time is 0.108.

Analysis of wind & demand power MAORDF-CapSA is shown in Figure 16. In left hand side of wind, then the value of time is 0.1. When the value of power is 7 then the value of time is 0.509. When the value of power is 10 then the value of time is 0.2. When the value of power is 12 then the value of time is 0.504. When the value of power is 15 then the value of time is 0.204. When the value of power is 17 then the value of time is 0.7. When the value of power is 20 then the value of time is 0.304. When the value of power is 21 then the value of time is 0.609. When the value of power is 24 then the value of time is 0.205. When the value of power is 7 then the value of time is 0.409. When the value of power is 10 then the value of time is 1. When the value of power is 12 then the value of time is 0.407. When the value of power is 15 then the value of time is 0.202. When the value of power is 17 then the value of time is 0.503. When the value of power is 20 then the value of time is 0.307. When the value of power is 21 then the value of time is 0.504. When the value of power is 24 then the value of time is 0.207. In right hand side of wind, when the value of power is 5 then the value of time is 0.1. When the value of power is 7 then the value of time is 2.1. When the value of power is 10 then the value of time is 0.2. When the value of power is 12 then the value of time is 2.1. When the value of power is 15 then the value of time is 0.4. When the value of power is 17 then the value of time is 3.8. When the value of power is 20 then the value of time is 0.3. When the value of power is 22 then the value of time is 3.7. When the value of power is 24 then the value of time is 0.3. In right hand side of demand, when the value of power is 5 then the value of time is 0.1. When the value of power is 7 then the value of time is 1.7. When the value of power is 10 then the value of time is 0.1. When the value of power is 12 then the value of time is 1.6. When the value of power is 15 then the value of time is 0.6. When the value of power is 17 then the value of time is 2.2. When the value of power is 20 then the value of time is 0.5. When the value of power is 22 then the value of time is 2.4. When the value of power is 24 then the value of time is 0.5.

Figure 17 despite the wind turbine and power. When the value of power is 5 then the value of time is 0.003. When the value of power is 8 then the

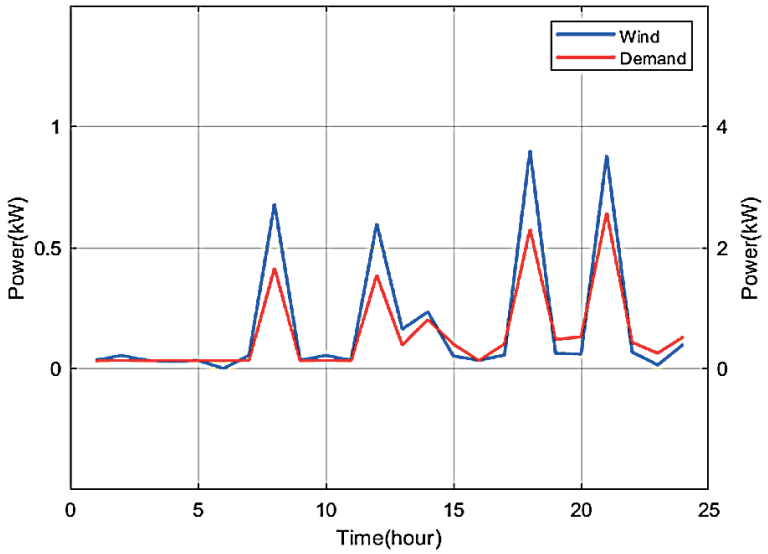

Figure 16. Analysis of wind & demand power MAORDF-CapSA

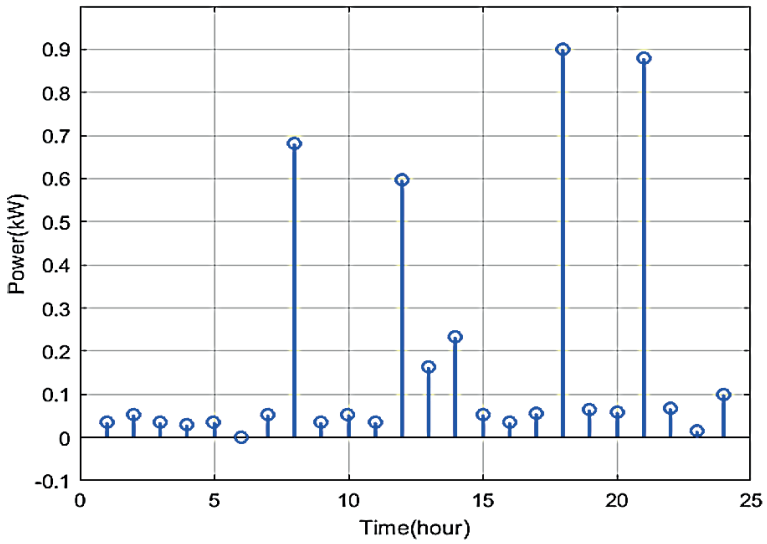

Figure 17. Wind turbine-power

value of time is 0.609. When the value of power is 10 then the value of time is 0.09. When the value of power is 12 then the value of time is 0.6. When the value of power is 15 then the value of time is 0.09. When the value of power is 18 then the value of time is 0.9. When the value of power is 20 then the value of time is 0.09. When the value of power is 21 then the value of time is 0.809. When the value of power is 24 then the value of time is 0.1. Analysis of home appliances rated power for 24-hour is shown on Table 1.

Table 1. Analysis of home appliances rated power for 24-hour

Appliance	Rated power (kW)	24-hours
Refrigerator	0.15	3.6
Iron	2.4	57.6
Toaster	0.708	16.992
Kettle	2	48
Hair dryer	1.536	36.864
LCD-TV	0.09	2.16
PC desktop	0.05	1.2
PC monitor	0.03	0.72
LED Lighting	0.035	0.84
Hair straightener	0.055	1.32
Oven	2.05	49.2
Dishwasher	1.7	40.8
Microwave oven	1.18	28.32
Printer	0.02	0.48
Air conditioner	1.14	27.36
Washing machine	1.8	43.2
Vacuum cleaner	1.9	45.6
Laptop	0.3	7.2

CONCLUSIONS

In this manuscript, IoT based smart home energy management system with power quality control in smart grid using MAORDF-CapSA technique is presented. The proposed controller is performed on MATLAB/Simulink working platform and its performances are analyzed with the existing systems. The performance of the proposed and the existing systems are graphically demonstrated. The existing systems are fruit fly optimization, fruit fly optimization and random decision optimization, Grasshopper optimization algorithm with particle swarm optimization aided artificial neural network, improved artificial bee colony, squirrel optimization with gravitational search-added neural network, radial basic function neural network oppositions crow search algorithm. The proposed hybrid technique is the combined execution of mexican axolotl optimization, random decision forest and capuchin search algorithm and hence it will be named as MAORDF-CapSA technique.

REFERENCES

1. Abdelaziz E.A., Saidur R., Mekhilef S. 2011. A review on energy saving strategies in industrial sector. Renewable and Sustainable Energy Reviews, 15(1), 150–168.
2. Ahmad S., Baig Z. 2012. Fuzzy-based optimization for effective detection of smart grid cyber-attacks. Int. J. Smart Grid Clean Energy, 1(1), 15–21.
3. Albert A., Rajagopal R. 2013. Smart meter driven segmentation: What your consumption says about

you. IEEE Transactions on Power Systems, 28(4), 4019–4030.

4. Bi Z., Da Xu L., Wang C. 2014. Internet of things for enterprise systems of modern manufacturing. IEEE Transactions on Industrial Informatics, 10(2), 1537–1546.
5. Çiçek A., Erenoğlu A.K., Erdinç O., Bozkurt A., Taşcıkaraoğlu A., Catalão J.P. 2021. Implementing a demand side management strategy for harmonics mitigation in a smart home using real measurements of household appliances.International Journal of Electrical Power & Energy Systems, 125, 106528.
6. Ding Y.M., Hong S.H., Li X.H. 2014. A demand response energy management scheme for industrial facilities in smart grid. IEEE Transactions on Industrial Informatics, 10(4), 2257–2269.
7. Duman A.C., Erden H.S., Gönül Ö., Güler Ö. 2021. A home energy management system with an integrated smart thermostat for demand response in smart grids. Sustainable Cities and Society, 65, 102639.
8. Erwinski K., Paprocki M., Grzesiak L.M., Karwowski K., Wawrzak A. 2012. Application of ethernetpowerlink for communication in a linuxrtai open cnc system. IEEE Transactions on Industrial Electronics, 60(2), 628–636.
9. Espinoza M., Joye C., Belmans R., De Moor B. 2005. Short-term load forecasting, profile identification, and customer segmentation: a methodology based on periodic time series. IEEE Transactions on Power Systems, 20(3), 1622–1630.
10. Ferrari P., Flammini A., Vitturi S. 2006. Performance analysis of PROFINET networks. Computer Standards & Interfaces, 28(4), 369–385.
11. Figueiredo V., Rodrigues F., Vale Z., Gouveia J.B. 2005. An electric energy consumer characterization framework based on data mining techniques. IEEE Transactions on power systems, 20(2), 596–602.
12. Jansen D., Buttner H. 2004. Real-time Ethernet: the EtherCAT solution. Computing and Control Engineering, 15(1), 16–21.
13. Javadi M.S., Nezhad A.E., Nardelli P.H., Gough M., Lotfi M., Santos S., Catalão J.P. 2021. Self-scheduling model for home energy management systems considering the end-users discomfort index within price-based demand response programs.Sustainable Cities and Society, 68, 102792.
14. Karthick T., Chandrasekaran K. 2021. Design of IoT based smart compact energy meter for monitoring and controlling the usage of energy and power quality issues with demand side management for a commercial building. Sustainable Energy, Grids and Networks, 26, 100454.
15. Kondili E., Pantelides C.C., Sargent R.W. 1993. A general algorithm for short-term scheduling of batch operations – I. MILP formulation. Computers & Chemical Engineering, 17(2), 211–227.
16. Marzband M., Ghadimi M., Sumper A., Domínguez-García J.L. 2014. Experimental validation of a real-time energy management system using multi-period gravitational search algorithm for microgrids in islanded mode. Applied Energy, 128, 164–174.
17. Marzband M., Sumper A., Domínguez-García J.L., Gumara-Ferret R. 2013. Experimental validation of a real time energy management system for microgrids in islanded mode using a local day-ahead electricity market and MINLP. Energy Conversion and Management, 76, 314–322.
18. Moro J.Z., Duarte L.F., Ferreira E.C., Dias J.A. 2013. A home appliance recognition system using the approach of measuring power consumption and power factor on the electrical panel, based on energy meter ICs. Circuits and Systems, 4(3), 245–251.
19. Neves D., Pina A., Silva C.A. 2015. Demand response modeling: A comparison between tools. Applied Energy, 146, 288–297.
20. Rao H., Shi X., Rodrigue A.K., Feng J., Xia Y., Elhoseny M., Yuan X., Gu L. 2019. Feature selection based on artificial bee colony and gradient boosting decision tree. Applied Soft Computing, 74, 634–642.
21. Rao H., Shi X., Rodrigue A.K., Feng J., Xia Y., Elhoseny M., Yuan X., Gu L. 2019. Feature selection based on artificial bee colony and gradient boosting decision tree. Applied Soft Computing, 74, 634–642.
22. Rehman A.U., Wadud Z., Elavarasan R.M., Hafeez G., Khan I., Shafiq Z., Alhelou H.H. 2021. An optimal power usage scheduling in smart grid integrated with renewable energy sources for energy management. IEEE Access, 9, 84619–84638.
23. Rodrigues Junior W.L., Borges F.A., Rabelo R.D., Rodrigues J.J., Fernandes R.A., da Silva I.N. 2021. A methodology for detection and classification of power quality disturbances using a real-time operating system in the context of home energy management systems. International Journal of Energy Research, 45(1), 203–219.
24. Siano P. 2014. Demand response and smart grids—A survey. Renewable and Sustainable Energy Reviews, 30, 461–478.
25. Suja K.R. 2021. Mitigation of power quality issues in smart grid using levy flight based moth flame optimization algorithm. Journal of Ambient Intelligence and Humanized Computing, 12(10), 9209–9228.
26. Tao F., Cheng Y., Da Xu L., Zhang L., Li B.H. 2014. CCIoT-CMfg: cloud computing and internet of things-based cloud manufacturing service system. IEEE Transactions on Industrial Informatics, 10(2), 1435–1442.
27. Tao F., Zuo Y., Da Xu L., Lv L., Zhang L. 2014.

Internet of things and BOM-based life cycle assessment of energy-saving and emission-reduction of products. IEEE Transactions on Industrial Informatics, 10(2), 1252–1261.

28. Trianni A., Cagno E., Farné S. 2016. Barriers, drivers and decision-making process for industrial energy efficiency: A broad study among manufacturing small and medium-sized enterprises. Applied Energy, 162, 1537–1551.
29. Villuendas-Rey Y., Velázquez-Rodríguez J.L., Alanis-Tamez M.D., Moreno-Ibarra M.A., Yáñez-Márquez C. 2021. Mexican axolotl optimization: a novel bioinspired heuristic. Mathematics, 9(7), 781.
30. Wang X., Mao X., Khodaei H. 2021. A multi-objective home energy management system based on internet of things and optimization algorithms. Journal of Building Engineering, 33, 101603.
31. Wu C.M., Chang R.S., Chan H.Y. 2014. A green energy-efficient scheduling algorithm using the DVFS technique for cloud datacenters. Future Generation Computer Systems, 37, 141–147.